Modeling of a Diesel Engine with VGT and EGR including Oxygen Mass Fraction

Johan Wahlström and Lars Eriksson

Vehicular systems
Department of Electrical Engineering
Linköpings universitet, SE-581 83 Linköping, Sweden
WWW: www.vehicular.isy.liu.se
E-mail: {johwa, larer}@isy.liu.se
Report: LiTH-ISY-R-2747

September 27, 2006

When citing this work, it is recommended that the citation is the improved and extended work, published in the peer-reviewed article Johan Wahlström and Lars Eriksson, Modeling diesel engines with a variable-geometry turbocharger and exhaust gas recirculation by optimization of model parameters for capturing non-linear system dynamics, Proceedings of the Institution of Mechanical Engineers, Part D, Journal of Automobile Engineering, Volume 225, Issue 7, July 2011, http://dx.doi.org/10.1177/0954407011398177.

Abstract

A mean value model of a diesel engine with VGT and EGR and that includes oxygen mass fraction is developed and validated. The intended model applications are system analysis, simulation, and development of model-based control systems. Model equations and tuning methods are described for each subsystem in the model. In order to decrease the amount of tuning parameters, flows and efficiencies are modeled using physical relationships and parametric models instead of look-up tables. The static models have mean relative errors that are equal to or lower than 6.1 %. Static and dynamic validations of the entire model show that the mean relative errors are less than 12 %. The validations also show that the proposed model captures the essential system properties, i.e. a non-minimum phase behavior in the transfer function EGR-valve to intake manifold pressure and a non-minimum phase behavior, an overshoot, and a sign reversal in the transfer function VGT to compressor mass flow.

Contents

1 Introduction

Legislated emission limits for heavy duty trucks are constantly reduced. To fulfill the requirements, technologies like Exhaust Gas Recirculation (EGR) systems and Variable Geometry Turbochargers (VGT) have been introduced. The primary emission reduction mechanisms utilized to control the emissions are that NO_x can be reduced by increasing the intake manifold EGR-fraction and smoke can be reduced by increasing the air/fuel ratio (Heywood, 1988). However the EGR fraction and air/fuel ratio depend in complicated ways on the EGR and VGT actuation. It is therefore necessary to have coordinated control of the EGR and VGT to reach the legislated emission limits in NO_x and smoke. When developing and validating a controller for this system, it is desirable to have a model that describes the system dynamics and the nonlinear effects. Therefore, the objective of this report is to construct a mean value diesel engine model with VGT and EGR. The model should be able to describe stationary operations and dynamics that are important for gas flow control. The intended usage of the model are system analysis, simulation and development of model-based control systems. In order to decrease the amount of tuning parameters, flows and efficiencies are modeled based upon physical relationships and parametric models instead of look-up tables. The model is implemented in MATLAB/SIMULINK using a component library.

1.1 Model structure

The structure of the model can be seen in Fig. 1. To be able to implement a model-based controller in a control system the model must be small. Therefore the model has only seven states: intake and exhaust manifold pressures (p_{im} and p_{em}), oxygen mass fraction in the intake and exhaust manifold (X_{Oim} and X_{Oem}), turbocharger speed (ω_t), and two states describing the actuator dynamics for the two control signals ($\tilde{u}_{egr}$ and $\tilde{u}_{vgt}$). These states are collected in a state vector x

$$x = (p_{im} \quad p_{em} \quad X_{Oim} \quad X_{Oem} \quad \omega_t \quad \tilde{u}_{egr} \quad \tilde{u}_{vgt})^T \tag{1}$$

Descriptions of the nomenclature, the variables and the indices can be found in Appendix A.

The modeling effort is focused on the gas flows, and it is important that the model can be utilized both for different vehicles and for engine testing, calibration, and certification in an engine test cell. In many of these situations the engine operation is defined by the rotational speed n_e, for example given as an input from a drivecycle, and therefore it is natural to parameterize the model using engine speed. The resulting model is thus expressed in state space form as

$$\dot{x} = f(x, u, n_e) \tag{2}$$

where the engine speed n_e is considered as an input to the model, and u is the control input vector

$$u = (u_\delta \quad u_{egr} \quad u_{vgt})^T \tag{3}$$

which contains mass of injected fuel u_δ, EGR-valve position u_{egr}, and VGT actuator position u_{vgt}. The EGR-valve is closed when $u_{egr} = 0\,\%$ and open when $u_{egr} = 100\,\%$. The VGT is closed when $u_{vgt} = 0\,\%$ and open when $u_{vgt} = 100\,\%$.

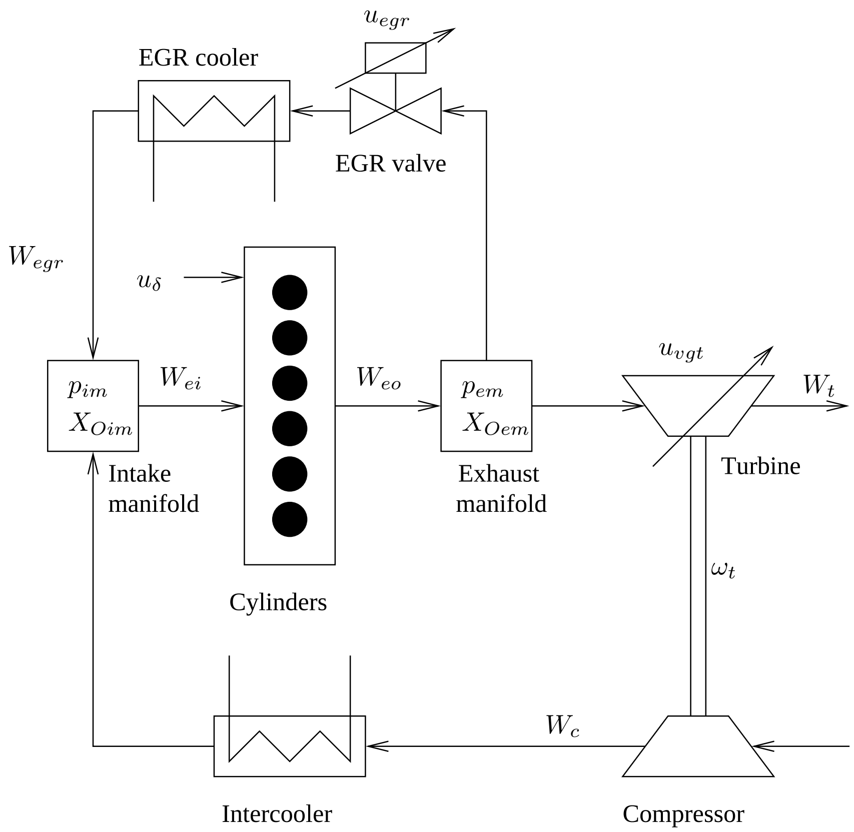

Figure 1: A model structure of the diesel engine. It has three control inputs and five main states related to the engine (p_{im}, p_{em}, X_{Oim}, X_{Oem}, and ω_t). In addition, there are two states for actuator dynamics ($\tilde{u}_{egr}$ and $\tilde{u}_{vgt}$).

1.2 Measurements

To tune and validate the model, stationary and dynamic measurements have been performed in an engine laboratory at Scania CV AB, and these are described below.

1.2.1 Stationary measurements

The stationary data consists of measurements at stationary conditions in 82 operating points, that are scattered over a large operating region covering different loads, speeds, VGT- and EGR-positions. These 82 operating points also include the European Stationary Cycle (ESC). The variables that were measured during stationary measurements can be seen in Tab. 1. The EGR fraction is calculated by measuring the carbon dioxide concentration in the intake and exhaust manifolds.

Table 1: Measured variables during stationary measurements.

Variable	Description	Unit
M_e	Engine torque	Nm
n_e	Rotational engine speed	rpm
n_t	Rotational turbine speed	rpm
p_{amb}	Ambient pressure	Pa
p_{em}	Exhaust manifold pressure	Pa
p_{im}	Intake manifold pressure	Pa
T_{amb}	Ambient temperature	K
T_c	Temperature after compressor	K
T_{em}	Exhaust manifold temperature	K
T_{im}	Intake manifold temperature	K
T_t	Temperature after turbine	K
u_{egr}	EGR control signal. 0 - closed, 100 - open	%
u_{vgt}	VGT control signal. 0 - closed, 100 - open	%
u_δ	Injected amount of fuel	$mg/cycle$
W_c	Compressor mass flow	kg/s
x_{egr}	EGR fraction	$-$

Table 2: Measured variables during dynamic measurements.

Variable	Description	Unit
M_e	Engine torque	Nm
n_e	Rotational engine speed	rpm
n_t	Rotational turbine speed	rpm
p_{em}	Exhaust manifold pressure	Pa
p_{im}	Intake manifold pressure	Pa
u_{egr}	EGR control signal. 0 - closed, 100 - open	%
u_{vgt}	VGT control signal. 0 - closed, 100 - open	%
u_δ	Injected amount of fuel	$mg/cycle$
W_c	Compressor mass flow	kg/s

1.2.2 Dynamic measurements

The dynamic data consists of measurements at dynamic conditions with steps in VGT control signal, EGR control signal, and fuel injection in several different operating points. The measurements are sampled with a frequency of 1 Hz, except for the steps in fuel injection where the measurements are sampled with a frequency of 10 Hz. These measurements are used in Sec. 8 for tuning of dynamic models and validation of the total engine model. The variables that were measured during dynamic measurements can be seen in Tab. 2.

1.3 Parameter estimation

Parameters in static models are estimated automatically using least squares optimization and data from stationary measurements. Parameters in dynamic models (volumes and an inertia) are estimated by adjusting these parameters manually until simulations of the complete model follow the dynamic responses in the dynamic measurements.

1.4 Relative error

Relative errors are calculated and used to evaluate the tuning and the validation of the model. Relative errors for stationary measurements between a measured variable $y_{meas,stat}$ and a modeled variable $y_{mod,stat}$ are calculated as

$$\text{stationary relative error}(i) = \frac{y_{meas,stat}(i) - y_{mod,stat}(i)}{\frac{1}{N}\sum_{i=1}^{N} y_{meas,stat}(i)} \tag{4}$$

where i is an operating point. Relative errors for dynamic measurements between a measured variable $y_{meas,dyn}$ and a modeled variable $y_{mod,dyn}$ are calculated as

$$\text{dynamic relative error}(j) = \frac{y_{meas,dyn}(j) - y_{mod,dyn}(j)}{\frac{1}{N}\sum_{i=1}^{N} y_{meas,stat}(i)} \tag{5}$$

where j is a time sample. In order to make a fair comparison between these relative errors, both the stationary and the dynamic relative error have the same stationary measurement in the denominator and the mean value of this stationary measurement is calculated in order to avoid large relative errors when $y_{meas,stat}$ is small.

1.5 Outline

The outline of the report is as follows. Sec. 2 describes the model equations for the intake and exhaust manifold. The cylinder flows, cylinder temperature, and cylinder torque are modeled in Sec. 3. In Sec. 4 a model of the EGR-valve is proposed and in Sec. 5 model equations for the turbocharger are described. The intercooler and EGR-cooler are modeled in Sec. 6. A summary of the model assumptions and the model equations is given in Sec. 7. Tuning and validation of the model are performed in Sec. 8. Finally, conclusions are drawn in Sec. 9.

2 Manifolds

The intake and exhaust manifolds are modeled as dynamic systems with two states each, pressure and oxygen mass fraction. The standard isothermal model (Heywood, 1988), that is based upon mass conservation, the ideal gas law, and that the manifold temperature is constant or varies slowly, has the differential equations for the manifold pressures

$$\begin{aligned} \frac{d}{dt}\, p_{im} &= \frac{R_a\, T_{im}}{V_{im}}\, (W_c + W_{egr} - W_{ei}) \\ \frac{d}{dt}\, p_{em} &= \frac{R_e\, T_{em}}{V_{em}}\, (W_{eo} - W_t - W_{egr}) \end{aligned} \tag{6}$$

There are two sets of thermodynamic properties: air has the ideal gas constant R_a and the specific heat capacity ratio γ_a, and exhaust gas has the ideal gas constant R_e and the specific heat capacity ratio γ_e. The intake manifold temperature T_{im} is assumed to be constant and equal to the cooling temperature in the intercooler, the exhaust manifold temperature T_{em} will be described in Sec. 3.2, and V_{im} and V_{em} are the manifold volumes. The mass flows W_c, W_{egr}, W_{ei}, W_{eo}, and W_t will be described in Sec. 3 to 5.

The EGR fraction in the intake manifold is calculated as

$$x_{egr} = \frac{W_{egr}}{W_c + W_{egr}} \tag{7}$$

Note that the EGR gas also contains oxygen that affects the oxygen fuel ratio in the cylinder. This effect is considered by modeling the oxygen concentrations X_{Oim} and X_{Oem} in the control volumes. These concentrations are defined as (Vigild, 2001)

$$X_{Oim} = \frac{m_{Oim}}{m_{totim}}, \quad X_{Oem} = \frac{m_{Oem}}{m_{totem}} \tag{8}$$

where m_{Oim} and m_{Oem} are the oxygen masses, and m_{totim} and m_{totem} are the total masses in the intake and exhaust manifolds. Differentiating X_{Oim} and X_{Oem} and using mass conservation (Vigild, 2001) give the following differential equations

$$\begin{aligned} \frac{d}{dt}\, X_{Oim} &= \frac{R_a\, T_{im}}{p_{im}\, V_{im}}\, ((X_{Oem} - X_{Oim})\, W_{egr} + (X_{Oc} - X_{Oim})\, W_c) \\ \frac{d}{dt}\, X_{Oem} &= \frac{R_e\, T_{em}}{p_{em}\, V_{em}}\, (X_{Oe} - X_{Oem})\, W_{eo} \end{aligned} \tag{9}$$

where X_{Oc} is the constant oxygen concentration in air passing the compressor, i.e. $X_{Oc} = 23.14\%$, and X_{Oe} is the oxygen concentration in the exhaust gases out from the engine cylinders, X_{Oe} will be described in Sec. 3.1.

Tuning parameters

- V_{im} and V_{em}: manifold volumes.

Tuning method

The tuning parameters V_{im} and V_{em} are obtained by adjusting these parameters manually until simulations of the complete model follow the dynamic responses in the dynamic measurements, see Sec. 8.1.

3 Cylinder

Three sub-models describe the behavior of the cylinder, these are:

- A mass flow model that models the flows through the cylinder, the oxygen to fuel ratio, and the oxygen concentration out from the cylinder.
- A model of the cylinder out temperature.
- A cylinder torque model.

3.1 Cylinder flow

The total mass flow W_{ei} into the cylinders is modeled using the volumetric efficiency η_{vol} (Heywood, 1988)

$$W_{ei} = \frac{\eta_{vol}\, p_{im}\, n_e\, V_d}{120\, R_a\, T_{im}} \tag{10}$$

where p_{im} and T_{im} are the pressure and temperature in the intake manifold, n_e is the engine speed and V_d is the displaced volume. The volumetric efficiency is in its turn modeled as

$$\eta_{vol} = c_{vol1}\sqrt{p_{im}} + c_{vol2}\sqrt{n_e} + c_{vol3} \tag{11}$$

The fuel mass flow W_f into the cylinders is controlled by u_δ, which gives the injected mass of fuel in mg per cycle and cylinder

$$W_f = \frac{10^{-6}}{120}\, u_\delta\, n_e\, n_{cyl} \tag{12}$$

where n_{cyl} is the number of cylinders. The mass flow W_{eo} out from the cylinder is given by the mass balance as

$$W_{eo} = W_f + W_{ei} \tag{13}$$

The oxygen to fuel ratio λ_O in the cylinder is defined as

$$\lambda_O = \frac{W_{ei}\, X_{Oim}}{W_f\, (O/F)_s} \tag{14}$$

where $(O/F)_s$ is the stoichiometric relation between oxygen and fuel masses.

During the combustion, the oxygen is burned in the presence of fuel. In diesel engines $\lambda_O > 1$ to avoid smoke. Therefore, it is assumed that $\lambda_O > 1$ and the oxygen concentration out from the cylinder can then be calculated as the unburned oxygen fraction

$$X_{Oe} = \frac{W_{ei}\, X_{Oim} - W_f\, (O/F)_s}{W_{eo}} \tag{15}$$

Tuning parameters

- c_{vol1}, c_{vol2}, c_{vol3}: volumetric efficiency constants

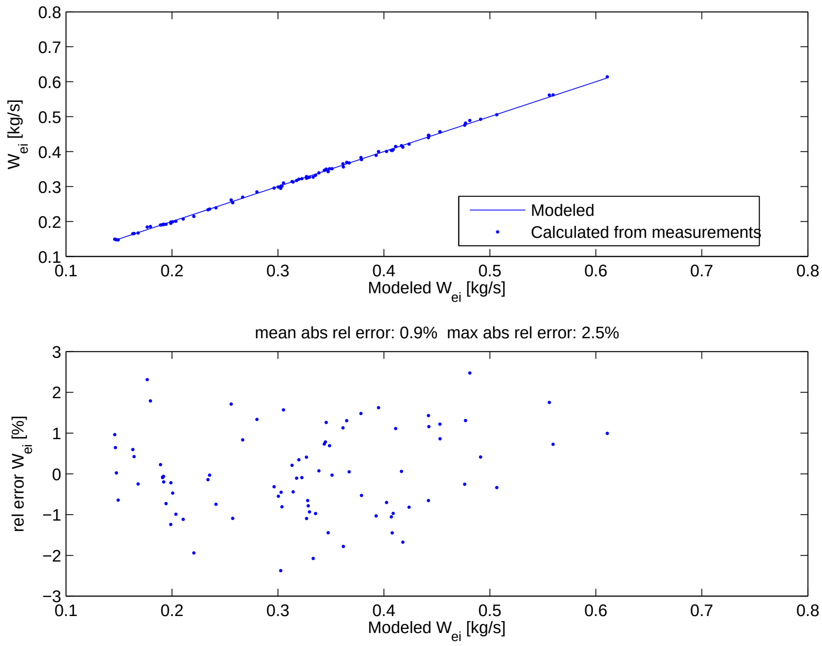

Figure 2: **Top:** Comparison of modeled mass flow W_{ei} into the cylinders and estimated W_{ei} from measurements. **Bottom:** Relative errors for modeled W_{ei} as function of modeled W_{ei} at steady state.

Tuning method

The tuning parameters c_{vol1}, c_{vol2}, and c_{vol3} are obtained by solving a linear least-squares problem that minimizes $(W_{ei} - W_{ei,meas})^2$ with c_{vol1}, c_{vol2}, and c_{vol3} as the optimization variables. The variable W_{ei} is the model in Eq. (10) and (11) and $W_{ei,meas}$ is estimated from stationary measurements as $W_{ei,meas} = W_c/(1 - x_{egr})$. Stationary measurements are used as inputs to the model during the tuning and the result can be seen in Fig. 2, which compares W_{ei} and $W_{ei,meas}$.

3.2 Cylinder out temperature

The cylinder out temperature T_e is modeled in the same way as in Skogtjärn (2002). This approach is based upon ideal gas Seliger cycle calculations that give the cylinder out temperature

$$T_e = \eta_{sc}\, \Pi_e^{1-1/\gamma_a}\, r_c^{1-\gamma_a}\, x_p^{1/\gamma_a - 1} \left(q_{in} \left(\frac{1 - x_{cv}}{c_{pa}} + \frac{x_{cv}}{c_{va}} \right) + T_1\, r_c^{\gamma_a - 1} \right) \tag{16}$$

where η_{sc} is a compensation factor for non ideal cycles and x_{cv} the ratio of fuel consumed during constant volume combustion. The rest of the fuel $(1 - x_{cv})$ is used during constant pressure combustion. Further, this model consists of the pressure quotient over the cylinder

$$\Pi_e = \frac{p_{em}}{p_{im}} \tag{17}$$

the pressure quotient between point 3 (after combustion) and point 2 (before combustion) in the Seliger cycle

$$x_p = \frac{p_3}{p_2} = 1 + \frac{q_{in}\, x_{cv}}{c_{va}\, T_1\, r_c^{\gamma_a - 1}} \tag{18}$$

the specific energy contents of the charge

$$q_{in} = \frac{W_f\, q_{HV}}{W_{ei} + W_f}\,(1 - x_r) \tag{19}$$

the temperature at inlet valve closing after intake stroke and mixing

$$T_1 = x_r\, T_e + (1 - x_r)\, T_{im} \tag{20}$$

the residual gas fraction

$$x_r = \frac{\Pi_e^{1/\gamma_a}\, x_p^{-1/\gamma_a}}{r_c\, x_v} \tag{21}$$

and the volume quotient between point 3 (after combustion) and point 2 (before combustion) in the Seliger cycle

$$x_v = \frac{v_3}{v_2} = 1 + \frac{q_{in}\,(1 - x_{cv})}{c_{pa}\left(\frac{q_{in}\, x_{cv}}{c_{va}} + T_1\, r_c^{\gamma_a - 1}\right)} \tag{22}$$

Since the equations above are non-linear and depend on each other, the cylinder out temperature is calculated numerically using a fixed point iteration which starts with the initial values $x_{r,0}$ and $T_{1,0}$. Then the following equations are applied in each iteration k

$$\begin{aligned}
q_{in,k+1} &= \frac{W_f\, q_{HV}}{W_{ei} + W_f}\,(1 - x_{r,k}) \\
x_{p,k+1} &= 1 + \frac{q_{in,k+1}\, x_{cv}}{c_{va}\, T_{1,k}\, r_c^{\gamma_a - 1}} \\
x_{v,k+1} &= 1 + \frac{q_{in,k+1}\,(1 - x_{cv})}{c_{pa}\left(\frac{q_{in,k+1}\, x_{cv}}{c_{va}} + T_{1,k}\, r_c^{\gamma_a - 1}\right)} \\
x_{r,k+1} &= \frac{\Pi_e^{1/\gamma_a}\, x_{p,k+1}^{-1/\gamma_a}}{r_c\, x_{v,k+1}} \\
T_{e,k+1} &= \eta_{sc}\, \Pi_e^{1-1/\gamma_a}\, r_c^{1-\gamma_a}\, x_{p,k+1}^{1/\gamma_a - 1}\left(q_{in,k+1}\left(\frac{1 - x_{cv}}{c_{pa}} + \frac{x_{cv}}{c_{va}}\right) + T_{1,k}\, r_c^{\gamma_a - 1}\right) \\
T_{1,k+1} &= x_{r,k+1}\, T_{e,k+1} + (1 - x_{r,k+1})\, T_{im}
\end{aligned} \tag{23}$$

In each sample during dynamic simulation, the initial values $x_{r,0}$ and $T_{1,0}$ are set to the solutions of x_r and T_1 from the previous sample.

Exhaust manifold temperature

The cylinder out temperature model above does not describe the exhaust manifold temperature completely due to heat losses. This is illustrated in Fig. 3(a) which shows a comparison between measured and modeled exhaust manifold temperature and in this figure it is assumed that the exhaust manifold temperature is equal to the cylinder out temperature, i.e. $T_{em} = T_e$. The relative error between model and measurement seems to increase from a negative error to a positive error for increasing mass flow W_{eo} out from the cylinder. The exhaust manifold temperature is measured in the exhaust manifold, thus the heat losses to the surroundings in the exhaust pipes between the cylinder and the exhaust manifold must be taken into consideration.

This temperature drop is modeled as a function of mass flow out from the cylinder, see Model 1 in Eriksson (2002).

$$T_{em} = T_{amb} + (T_e - T_{amb})\, e^{-\frac{h_{tot}\,\pi\, d_{pipe}\, l_{pipe}\, n_{pipe}}{W_{eo}\, c_{pe}}} \tag{24}$$

where T_{amb} is the ambient temperature, h_{tot} the total heat transfer coefficient, d_{pipe} the pipe diameter, l_{pipe} the pipe length and n_{pipe} the number of pipes. Using this model, the mean and maximum absolute relative error is reduced, see Fig. 3(b).

Approximating the solution to the cylinder out temperature

As explained above, the cylinder out temperature is calculated numerically using the fixed point iteration Eq. (23). Fig. 4 shows that it is sufficient to use one iteration in this iterative process. This is shown by comparing the solution from one iteration with one that has a sufficient number of iterations to give a solution with 0.01 % accuracy. The maximum absolute relative error of the solution from one iteration (compared to the solution with 0.01 % accuracy) is 0.15 %. This error is small because the fixed point iteration Eq. (23) has initial values that are close to the solution. Consequently, it is sufficient to use one iteration in this model since the mean absolute relative error of the exhaust manifold temperature model (compared to the measurements in Fig. 3(b)) is 1.7 %.

Tuning parameters

- η_{sc}: compensation factor for non ideal cycles
- x_{cv}: the ratio of fuel consumed during constant volume combustion
- h_{tot}: the total heat transfer coefficient

Tuning method

The tuning parameters η_{sc}, x_{cv}, and h_{tot} are obtained by solving a non-linear least-squares problem that minimizes $(T_{em} - T_{em,meas})^2$ with η_{sc}, x_{cv}, and h_{tot} as the optimization variables. The variable T_{em} is the model in Eq. (23) and (24) with stationary measurements as inputs to the model, and $T_{em,meas}$ is a stationary measurement. The result of the tuning is shown in Fig. 3(b).

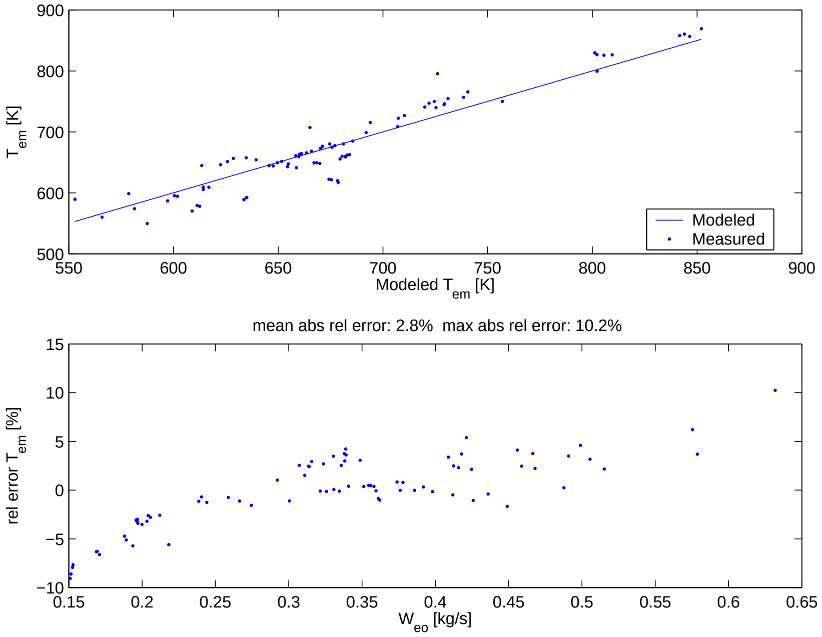

(a) Without a model for heat losses in the exhaust pipes, i.e. $T_{em} = T_e$.

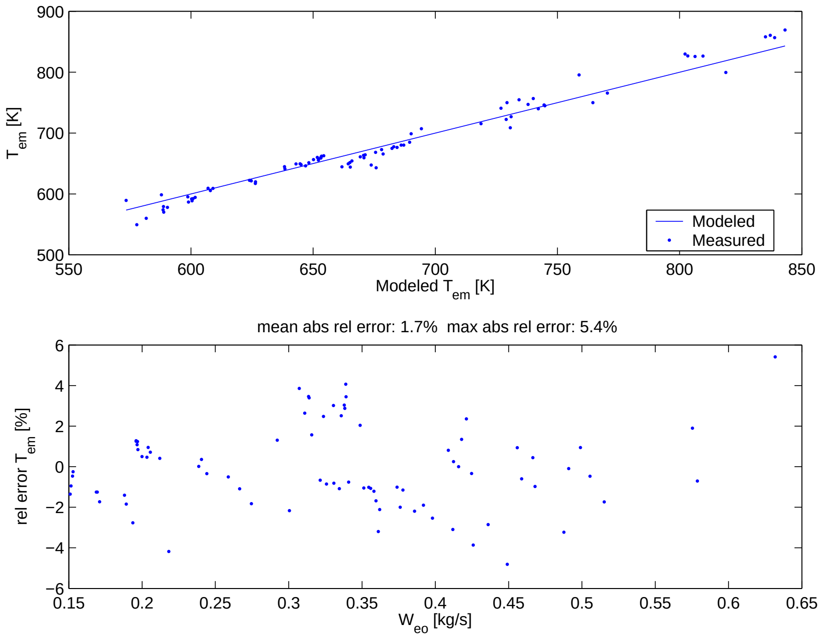

(b) With model (24) for heat losses in the exhaust pipes.

Figure 3: Modeled and measured exhaust manifold temperature T_{em} and relative errors for modeled T_{em} at steady state.

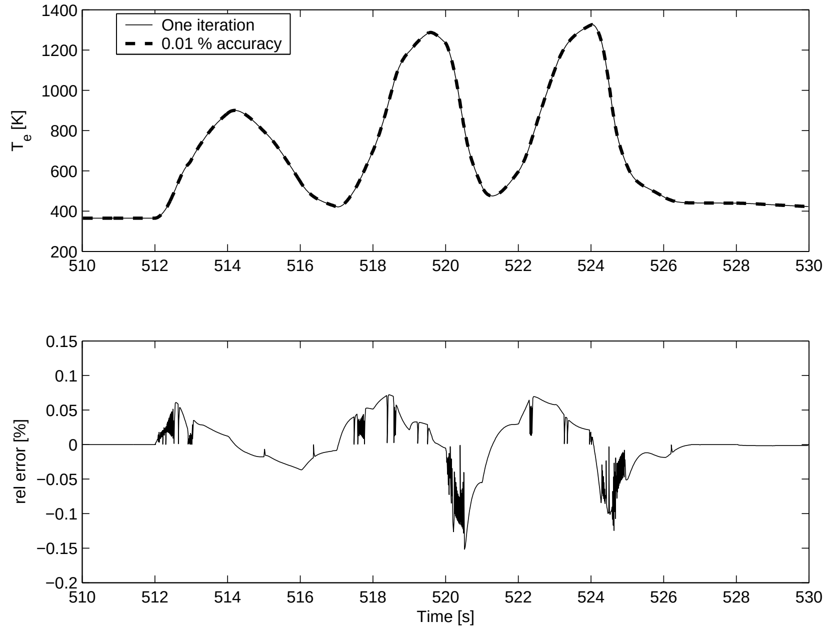

Figure 4: The cylinder out temperature T_e is calculated by simulating the total engine model during the complete European Transient Cycle. This figure shows the part of the European Transient Cycle that consists of the maximum relative error. **Top:** The fixed point iteration Eq. (23) is used in two ways: by using one iteration and to get 0.01 % accuracy. **Bottom:** Relative errors between the solutions from one iteration and 0.01 % accuracy.

3.3 Cylinder torque

The torque produced by the engine M_e is modeled using three different engine components; the gross indicated torque M_{ig}, the pumping torque M_p, and the friction torque M_{fric} (Heywood, 1988).

$$M_e = M_{ig} - M_p - M_{fric} \tag{25}$$

The pumping torque is modeled using the intake and exhaust manifold pressures.

$$M_p = \frac{V_d}{4\,\pi}\,(p_{em} - p_{im}) \tag{26}$$

The gross indicated torque is coupled to the energy that comes from the fuel

$$M_{ig} = \frac{u_\delta\,10^{-6}\,n_{cyl}\,q_{HV}\,\eta_{ig}}{4\,\pi} \tag{27}$$

Assuming that the engine is always running at optimal injection timing, the gross indicated efficiency η_{ig} is modeled as

$$\eta_{ig} = \eta_{igch}\left(1 - \frac{1}{r_c^{\gamma_{cyl}-1}}\right) \tag{28}$$

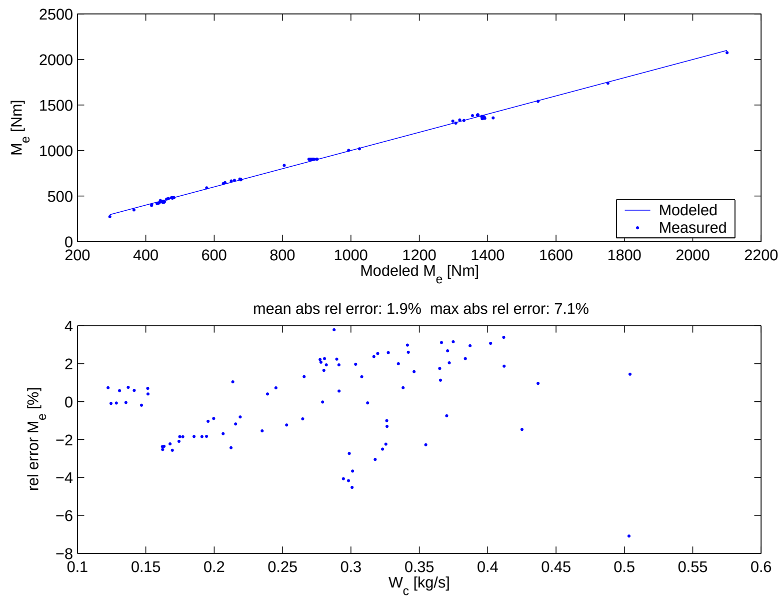

Figure 5: Comparison of measurements and model for the engine torque M_e at steady state. **Top:** Modeled and measured engine torque M_e. **Bottom:** Relative errors for modeled M_e.

where the parameter η_{igch} is estimated from measurements, r_c is the compression ratio, and γ_{cyl} is the specific heat capacity ratio for the gas in the cylinder. The friction torque is assumed to follow a polynomial function

$$M_{fric} = \frac{V_d}{4\,\pi} 10^5 \, \left(c_{fric1} \, n_{eratio}^2 + c_{fric2} \, n_{eratio} + c_{fric3} \right) \tag{29}$$

where

$$n_{eratio} = \frac{n_e}{1000} \tag{30}$$

Tuning model parameters

- η_{igch}: combustion chamber efficiency
- c_{fric1}, c_{fric2}, c_{fric3}: coefficients in the polynomial function for the friction torque

Tuning method

The tuning parameters η_{igch}, c_{fric1}, c_{fric2}, and c_{fric3} are obtained by solving a linear least-squares problem that minimizes $(M_e + M_p - M_{e,meas} - M_{p,meas})^2$ with the tuning parameters as the optimization variables. The model of $M_e + M_p$ is obtained by solving $M_e + M_p$ from Eq. (25) and $M_{e,meas} + M_{p,meas}$ is estimated from stationary measurements as $M_{e,meas} + M_{p,meas} = M_e + V_d(p_{em} - p_{im})/(4\pi)$. Stationary measurements are used as inputs to the model. The result of the tuning can be seen in Fig. 5.

4 EGR-valve

The mass flow through the EGR-valve is modeled as a simplification of a compressible flow restriction with variable area (Heywood, 1988) and with the assumption that there is no reverse flow when $p_{em} < p_{im}$. The motive for this assumption is to construct a simple model. The model can be extended with reverse flow, but this increases the complexity of the model since a reverse flow model requires mixing of different temperatures and oxygen fractions in the exhaust manifold and a change of the temperature and the gas constant in the EGR mass flow model. However, p_{em} is larger than p_{im} in normal operating points, consequently the assumption above will not effect the model behavior in these operating points. Furthermore, reverse flow is not measured and can therefore not be validated.

The mass flow through the restriction is

$$W_{egr} = \frac{A_{egr}\, p_{em}\, \Psi_{egr}}{\sqrt{T_{em}\, R_e}} \tag{31}$$

where

$$\Psi_{egr} = \sqrt{\frac{2\,\gamma_e}{\gamma_e - 1}\left(\mathit{\Pi}_{egr}^{2/\gamma_e} - \mathit{\Pi}_{egr}^{1+1/\gamma_e}\right)} \tag{32}$$

Measurement data shows that Eq. (32) does not give a sufficiently accurate description of the EGR flow. Pressure pulsations in the exhaust manifold or the influence of the EGR-cooler could be two different explanations for this phenomenon. In order to maintain the density influence $(p_{em}/(\sqrt{T_{em}\, R_e}))$ in Eq. (31) and the simplicity in the model, the function Ψ_{egr} is instead modeled as a parabolic function (see Fig. 6 where Ψ_{egr} is plotted as function of Π_{egr}).

$$\Psi_{egr} = 1 - \left(\frac{1 - \Pi_{egr}}{1 - \Pi_{egropt}} - 1\right)^2 \tag{33}$$

The pressure quotient Π_{egr} over the valve is limited when the flow is choked, i.e. when sonic conditions are reached in the throat, and when $1 < p_{im}/p_{em}$, i.e. no backflow can occur.

$$\mathit{\Pi}_{egr} = \begin{cases} \Pi_{egropt} & \text{if } \frac{p_{im}}{p_{em}} < \Pi_{egropt} \\ \frac{p_{im}}{p_{em}} & \text{if } \Pi_{egropt} \leq \frac{p_{im}}{p_{em}} \leq 1 \\ 1 & \text{if } 1 < \frac{p_{im}}{p_{em}} \end{cases} \tag{34}$$

For a compressible flow restriction, the standard model for Π_{egropt} is

$$\Pi_{egropt} = \left(\frac{2}{\gamma_e + 1}\right)^{\frac{\gamma_e}{\gamma_e - 1}} \tag{35}$$

but the accuracy of the EGR flow model is improved by replacing the physical value of Π_{egropt} in Eq. (35) with a tuning parameter (Andersson, 2005).

The effective area

$$A_{egr} = A_{egrmax}\, f_{egr}(\tilde{u}_{egr}) \tag{36}$$

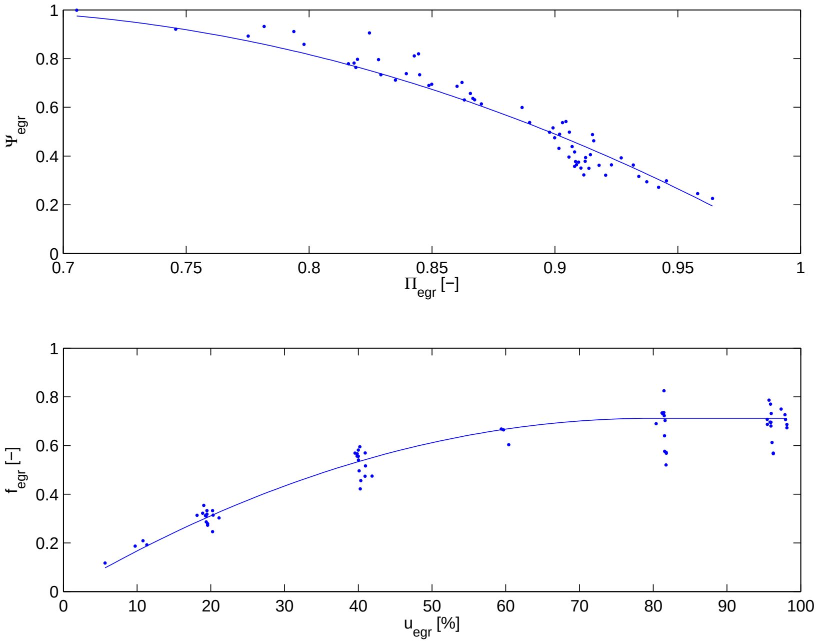

Figure 6: Comparison of estimated points from measurements and two sub-models for the EGR flow W_{egr} at steady state showing how different variables in the sub-models depend on each other. Note that this is not a validation of the sub-models since the estimated points for the sub-models depend on the model tuning. **Top:** Ψ_{egr} as function of pressure quotient Π_{egr}. The estimated points are calculated by solving Ψ_{egr} from Eq. (31). The model is described by Eq. (33). **Bottom:** Effective area ratio f_{egr} as function of control signal u_{egr}. The estimated points are calculated by solving f_{egr} from Eq. (31). The model is described by Eq. (37).

is modeled as a polynomial function of the EGR valve position $\tilde{u}_{egr}$ (see Fig. 6 where f_{egr} is plotted as function of u_{egr})

$$f_{egr}(\tilde{u}_{egr}) = \begin{cases} c_{egr1}\,\tilde{u}_{egr}^2 + c_{egr2}\,\tilde{u}_{egr} + c_{egr3} & \text{if } \tilde{u}_{egr} \leq -\frac{c_{egr2}}{2\,c_{egr1}} \\ c_{egr3} - \frac{c_{egr2}^2}{4\,c_{egr1}} & \text{if } \tilde{u}_{egr} > -\frac{c_{egr2}}{2\,c_{egr1}} \end{cases} \tag{37}$$

where $\tilde{u}_{egr}$ describes the EGR actuator dynamic

$$\frac{d}{dt}\,\tilde{u}_{egr} = \frac{1}{\tau_{egr}}(u_{egr}(t - \tau_{degr}) - \tilde{u}_{egr}) \tag{38}$$

The EGR-valve is open when $\tilde{u}_{egr} = 100\%$ and closed when $\tilde{u}_{egr} = 0\%$. The values of τ_{egr} and τ_{degr} have been provided by industry.

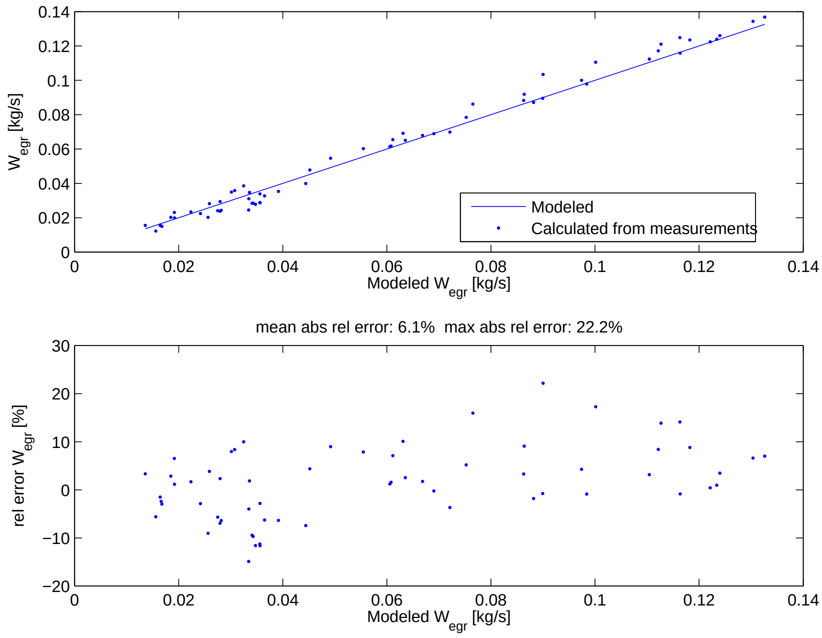

Figure 7: **Top:** Comparison between modeled EGR flow W_{egr} and estimated W_{egr} from measurements at steady state. **Bottom:** Relative errors for W_{egr} at steady state.

Tuning parameters

- Π_{egropt}: optimal value of Π_{egr} for maximum value of the function Ψ_{egr} in Eq. (33)
- c_{egr1}, c_{egr2}, c_{egr3}: coefficients in the polynomial function for the effective area

Tuning method

The tuning parameter Π_{egropt} is obtained by solving a non-linear least-squares problem that minimizes $(W_{egr} - W_{egr,meas})^2$ with Π_{egropt} as the optimization variable. In each iteration in the non-linear least-squares solver, the values for c_{egr1}, c_{egr2}, and c_{egr3} are set to be the solution of a linear least-squares problem that minimizes $(W_{egr} - W_{egr,meas})^2$ for the current value of Π_{egropt}. The variable W_{egr} is described by the model Eq. (31) and $W_{egr,meas}$ is estimated from measurements as $W_{egr,meas} = W_c\, x_{egr}/(1 - x_{egr})$. Stationary measurements are used as inputs to the model. The result of the tuning is shown in Fig. 7.

5 Turbocharger

The turbocharger consist of a turbo inertia model, a turbine model, and a compressor model.

5.1 Turbo inertia

For the turbo speed ω_t, Newton's second law gives

$$\frac{d}{dt}\omega_t = \frac{P_t\,\eta_m - P_c}{J_t\,\omega_t} \tag{39}$$

where J_t is the inertia, P_t is the power delivered by the turbine, P_c is the power required to drive the compressor, and η_m is the mechanical efficiency in the turbocharger.

Tuning parameter

- J_t: turbo inertia

Tuning method

The tuning parameter J_t is obtained by adjusting this parameter manually until simulations of the complete model follow the dynamic responses in the dynamic measurements, see Sec. 8.1.

5.2 Turbine

The turbine models are the total turbine efficiency and the turbine mass flow.

5.2.1 Turbine efficiency

One way to model the power P_t is to use the turbine efficiency η_t, which is defined as (Heywood, 1988)

$$\eta_t = \frac{P_t}{P_{t,s}} = \frac{T_{em} - T_t}{T_{em}(1 - \Pi_t^{1-1/\gamma_e})} \tag{40}$$

where T_t is the temperature after the turbine, Π_t is the pressure ratio

$$\Pi_t = \frac{p_{amb}}{p_{em}} \tag{41}$$

and $P_{t,s}$ is the power from the isentropic process

$$P_{t,s} = W_t\, c_{pe}\, T_{em}\left(1 - \Pi_t^{1-1/\gamma_e}\right) \tag{42}$$

where W_t is the turbine mass flow.

However, Eq. (40) is not applicable due to heat losses in the turbine which cause temperature drops in the temperatures T_t and T_{em}. Consequently, there will be errors for η_t if Eq. (40) is used to calculate η_t from measurements. One way to overcome this is to model the temperature drops, but it is difficult to tune these models since there exists no measurements of these temperature drops.

Another way to overcome this, that is frequently used in the literature, is to use another efficiency that are approximatively equal to η_t. This approximation utilizes that

$$P_t\,\eta_m = P_c \tag{43}$$

at steady state according to Eq. (39). Consequently, $P_t \approx P_c$ at steady state. Using this approximation in Eq. (40), another efficiency η_{tm} is obtained

$$\eta_{tm} = \frac{P_c}{P_{t,s}} = \frac{W_c\, c_{pa}(T_c - T_{amb})}{W_t\, c_{pe}\, T_{em}\left(1 - \Pi_t^{1-1/\gamma_e}\right)} \tag{44}$$

where T_c is the temperature after the compressor and W_c is the compressor mass flow. The temperature T_{em} in Eq. (44) introduces less errors compared to the temperature difference $T_{em} - T_t$ in Eq. (40) due to that the absolute value of T_{em} is larger than the absolute value of $T_{em} - T_t$. Consequently, Eq. (44) introduces less errors compared to Eq. (40) since Eq. (44) does not consist of $T_{em} - T_t$. The temperatures T_c and T_{amb} are low and they introduce less errors compared to T_{em} and T_t since the heat losses in the compressor are comparatively small. Another advantage of using Eq. (44) is that the individual variables P_t and η_m in Eq. (39) do not have to be modeled. Instead, the product $P_t\,\eta_m$ is modeled using Eq. (43) and (44)

$$P_t\,\eta_m = P_c = \eta_{tm}\, P_{t,s} = \eta_{tm}\, W_t\, c_{pe}\, T_{em}\left(1 - \Pi_t^{1-1/\gamma_e}\right) \tag{45}$$

Measurements show that η_{tm} depends on the blade speed ratio (BSR) as a parabolic function (Watson and Janota, 1982), see Fig. 8 where η_{tm} is plotted as function of BSR.

$$\eta_{tm} = \eta_{tm,max} - c_m(BSR - BSR_{opt})^2 \tag{46}$$

The blade speed ratio is the quotient of the turbine blade tip speed and the speed which a gas reaches when expanded isentropically at the given pressure ratio Π_t

$$BSR = \frac{R_t\,\omega_t}{\sqrt{2\, c_{pe}\, T_{em}\left(1 - \Pi_t^{1-1/\gamma_e}\right)}} \tag{47}$$

where R_t is the turbine blade radius. The parameter c_m in the parabolic function varies due to mechanical losses and c_m is therefore modeled as a function of the turbo speed

$$c_m = c_{m1}(\omega_t - c_{m2})^{c_{m3}} \tag{48}$$

see Fig. 8 where c_m is plotted as function of ω_t.

Tuning parameters

- $\eta_{tm,max}$: maximum turbine efficiency
- BSR_{opt}: optimum BSR value for maximum turbine efficiency
- c_{m1}, c_{m2}, c_{m3}: parameters in the model for c_m

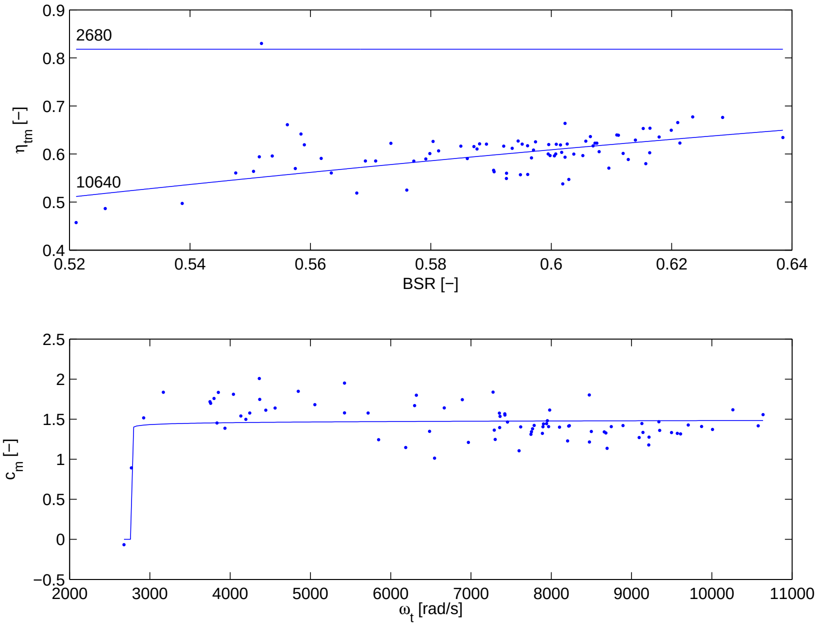

Figure 8: Comparison of estimated points from measurements and the model for the turbine efficiency η_{tm} at steady state. **Top:** η_{tm} as function of blade speed ratio BSR. The estimated points are calculated by using Eq. (44) and (47). The model Eq. (46) is plotted at two different turbo speeds ω_t. **Bottom:** Parameter c_m as function of turbo speed ω_t. The estimated points are calculated by solving c_m from Eq. (46). The model is described by Eq. (48). Note that this plot is not a validation of c_m since the estimated points for c_m depend on the model tuning.

Tuning method

The tuning parameters BSR_{opt}, c_{m2}, and c_{m3} are obtained by solving a non-linear least-squares problem that minimizes $(\eta_{tm} - \eta_{tm,meas})^2$ with BSR_{opt}, c_{m2}, and c_{m3} as the optimization variables. In each iteration in the non-linear least-squares solver, the values for $\eta_{tm,max}$ and c_{m1} are set to be the solution of a linear least-squares problem that minimizes $(\eta_{tm} - \eta_{tm,meas})^2$ for the current values of BSR_{opt}, c_{m2}, and c_{m3}. The efficiency η_{tm} is described by the model Eq. (46) and $\eta_{tm,meas}$ is estimated from measurements using Eq. (44). Stationary measurements are used as inputs to the model. The result of the tuning is shown in Fig. 8 and 9.

5.2.2 Turbine mass flow

The turbine mass flow W_t is modeled using the corrected mass flow (Heywood, 1988; Watson and Janota, 1982)

$$\frac{W_t \sqrt{T_{em}}}{p_{em}} = A_{vgtmax}\, f_{\Pi t}(\Pi_t)\, f_{vgt}(\tilde{u}_{vgt}) \tag{49}$$

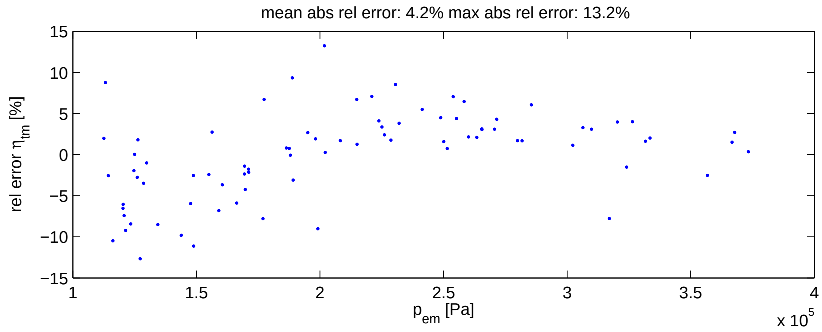

Figure 9: Relative errors for the total turbine efficiency η_{tm} as function of exhaust manifold pressure p_{em} at steady state.

where A_{vgtmax} is the maximum area in the turbine that the gas flows through. Measurements show that the corrected mass flow depends on the pressure ratio Π_t and the VGT actuator signal $\tilde{u}_{vgt}$. As the pressure ratio decreases, the corrected mass flow increases until the gas reaches the sonic condition and the flow is choked. This behavior can be described by a choking function

$$f_{\Pi t}(\Pi_t) = \sqrt{1 - \Pi_t^{K_t}} \tag{50}$$

which is not based on the physics of the turbine, but it gives good agreement with measurements using few parameters (Eriksson et al., 2002), see Fig. 10 where $f_{\Pi t}$ is plotted as function of Π_t.

When the VGT control signal u_{vgt} increases, the effective area increases and hence also the flow increases. Due to the geometry in the turbine, the change in effective area is large when the VGT control signal is large. This behavior can be described by a part of an ellipse (see Fig. 10 where f_{vgt} is plotted as function of u_{vgt})

$$\left(\frac{f_{vgt}(\tilde{u}_{vgt}) - c_{f2}}{c_{f1}}\right)^2 + \left(\frac{\tilde{u}_{vgt} - c_{vgt2}}{c_{vgt1}}\right)^2 = 1 \tag{51}$$

where f_{vgt} is the effective area ratio function and $\tilde{u}_{vgt}$ describes the VGT actuator dynamic

$$\frac{d}{dt}\,\tilde{u}_{vgt} = \frac{1}{\tau_{vgt}}(u_{vgt} - \tilde{u}_{vgt}) \tag{52}$$

The value of τ_{vgt} has been provided by industry. The flow can now be modeled by solving W_t from Eq. (49)

$$W_t = \frac{A_{vgtmax}\, p_{em}\, f_{\Pi t}(\Pi_t)\, f_{vgt}(\tilde{u}_{vgt})}{\sqrt{T_{em}}} \tag{53}$$

and solving f_{vgt} from Eq. (51)

$$f_{vgt}(\tilde{u}_{vgt}) = c_{f2} + c_{f1}\sqrt{1 - \left(\frac{\tilde{u}_{vgt} - c_{vgt2}}{c_{vgt1}}\right)^2} \tag{54}$$

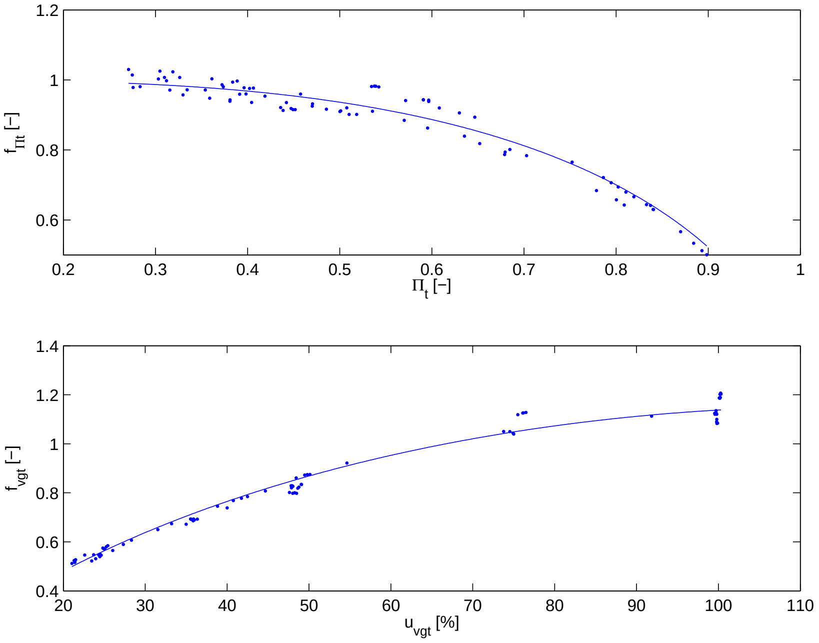

Figure 10: Comparison of estimated points from measurements and two sub-models for the turbine mass flow at steady state showing how different variables in the sub-models depend on each other. Note that this is not a validation of the sub-models since the estimated points for the sub-models depend on the model tuning. **Top:** The choking function $f_{\Pi t}$ as function of the pressure ratio Π_t. The estimated points are calculated by solving $f_{\Pi t}$ from Eq. (49). The model is described by Eq. (50). **Bottom:** The effective area ratio function f_{vgt} as function of the control signal u_{vgt}. The estimated points are calculated by solving f_{vgt} from Eq. (49). The model is described by Eq. (54).

Tuning parameters

- K_t: exponent in the choking function for the turbine flow
- c_{f1}, c_{f2}, c_{vgt1}, c_{vgt2}: parameters in the ellipse for the effective area ratio function

Tuning method

The tuning parameters above are obtained by solving a non-linear least-squares problem that minimizes $(W_t - W_{t,meas})^2$ with the tuning parameters as the optimization variables. The flow W_t is described by the model Eq. (53), (54), and (50), and $W_{t,meas}$ is estimated from measurements as $W_{t,meas} = W_c + W_f$, where W_f is estimated using Eq. (12). Stationary measurements are used as inputs to the model. The result of the tuning is shown in Fig. 11.

5.3 Compressor

The compressor models the compressor efficiency and the compressor mass flow.

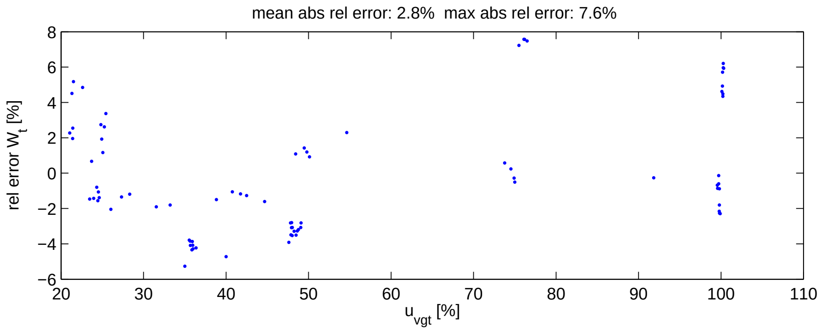

Figure 11: Relative errors for turbine flow W_t as function of control signal u_{vgt} at steady state.

5.3.1 Compressor efficiency

The compressor power P_c is modeled using the compressor efficiency η_c, which is defined as (Heywood, 1988)

$$\eta_c = \frac{P_{c,s}}{P_c} = \frac{T_{amb}\left(\Pi_c^{1-1/\gamma_a} - 1\right)}{T_c - T_{amb}} \tag{55}$$

where T_c is the temperature after the compressor, Π_c is the pressure ratio

$$\Pi_c = \frac{p_{im}}{p_{amb}} \tag{56}$$

and $P_{c,s}$ is the power from the isentropic process

$$P_{c,s} = W_c\, c_{pa}\, T_{amb}\left(\Pi_c^{1-1/\gamma_a} - 1\right) \tag{57}$$

where W_c is the compressor mass flow. The power P_c is modeled by solving P_c from Eq. (55) and using Eq. (57)

$$P_c = \frac{P_{c,s}}{\eta_c} = \frac{W_c\, c_{pa}\, T_{amb}}{\eta_c}\left(\Pi_c^{1-1/\gamma_a} - 1\right) \tag{58}$$

The efficiency is modeled using ellipses similar to Guzzella and Amstutz (1998), but with a non-linear transformation on the axis for the pressure ratio. The inputs to the efficiency model are Π_c and W_c (see Fig. 16). The flow W_c is not scaled by the inlet temperature and the inlet pressure since these two variables are constant. The ellipses can be described as

$$\eta_c = \eta_{cmax} - \chi^T\, Q_c\, \chi \tag{59}$$

χ is a vector which contains the inputs

$$\chi = \begin{bmatrix} W_c - W_{copt} \\ \pi_c - \pi_{copt} \end{bmatrix} \tag{60}$$

where the non-linear transformation for Π_c is

$$\pi_c = (\Pi_c - 1)^{pow_\pi} \tag{61}$$

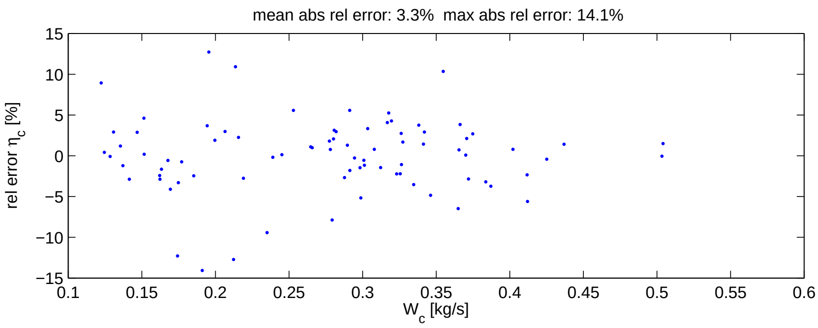

Figure 12: Relative errors for η_c as function of W_c at steady state.

and the symmetric matrix Q_c consists of three parameters

$$Q_c = \begin{bmatrix} a_1 & a_3 \\ a_3 & a_2 \end{bmatrix} \tag{62}$$

Tuning model parameters

- η_{cmax}: maximum compressor efficiency
- W_{copt} and π_{copt}: optimum values of W_c and π_c for maximum compressor efficiency
- pow_π: exponent in the scale function, Eq. (61)
- a_1, a_2 and a_3: parameters in the matrix Q_c

Tuning method

The tuning parameters W_{copt}, π_{copt}, and pow_π are obtained by solving a non-linear least-squares problem that minimizes $(\eta_c - \eta_{c,meas})^2$ with W_{copt}, π_{copt}, and pow_π as the optimization variables. In each iteration in the non-linear least-squares solver, the values for η_{cmax}, a_1, a_2 and a_3 are set to be the solution of a linear least-squares problem that minimizes $(\eta_c - \eta_{c,meas})^2$ for the current values of W_{copt}, π_{copt}, and pow_π. The efficiency η_c is described by the model Eq. (59) to (62) and $\eta_{c,meas}$ is estimated from measurements using Eq. (55). Stationary measurements are used as inputs to the model. The result of the tuning is shown in Fig. 12.

5.3.2 Compressor mass flow

The mass flow W_c through the compressor is modeled using two dimensionless variables. The first variable is the energy transfer coefficient (Dixon, 1998)

$$\Psi_c = \frac{2\, c_{pa}\, T_{amb} \left(\Pi_c^{1-1/\gamma_a} - 1\right)}{R_c^2\, \omega_t^2} \tag{63}$$

which is the quotient of the isentropic kinetic energy of the gas at the given pressure ratio Π_c and the kinetic energy of the compressor blade tip where R_c

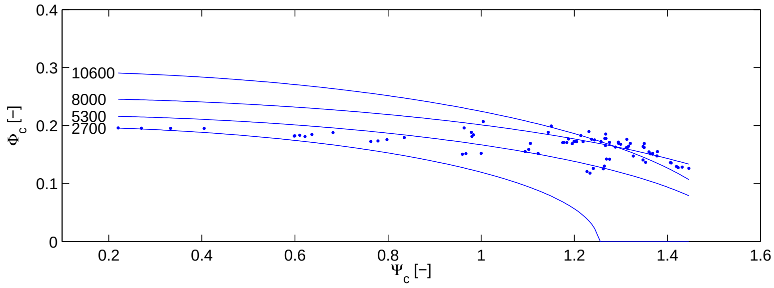

Figure 13: Comparison of estimated points from measurements and model for the compressor mass flow W_c at steady state. Volumetric flow coefficient Φ_c as function of energy transfer coefficient Ψ_c. The estimated points are calculated using Eq. (63) and (64). The model (Eq. 68) is plotted at four different turbo speeds ω_t.

is compressor blade radius. The second variable is the volumetric flow coefficient (Dixon, 1998)

$$\Phi_c = \frac{W_c/\rho_{amb}}{\pi\, R_c^3\, \omega_t} = \frac{R_a\, T_{amb}}{p_{amb}\, \pi\, R_c^3\, \omega_t} W_c \tag{64}$$

which is the quotient of volume flow rate of air into the compressor and the rate at which volume is displaced by the compressor blade where ρ_{amb} is the density of the ambient air. The relation between Ψ_c and Φ_c can be described by a part of an ellipse (Andersson, 2005), see Fig. 13 where Φ_c is plotted as function of Ψ_c.

$$c_{\Psi 1}(\omega_t)\,(\Psi_c - c_{\Psi 2})^2 + c_{\Phi 1}(\omega_t)\,(\Phi_c - c_{\Phi 2})^2 = 1 \tag{65}$$

where $c_{\Psi 1}$ and $c_{\Phi 1}$ varies with turbo speed ω_t and are modeled as polynomial functions.

$$c_{\Psi 1}(\omega_t) = c_{\omega\Psi 1}\,\omega_t^2 + c_{\omega\Psi 2}\,\omega_t + c_{\omega\Psi 3} \tag{66}$$

$$c_{\Phi 1}(\omega_t) = c_{\omega\Phi 1}\,\omega_t^2 + c_{\omega\Phi 2}\,\omega_t + c_{\omega\Phi 3} \tag{67}$$

In Fig. 14 the variables $c_{\Psi 1}$ and $c_{\Phi 1}$ are plotted as function of the turbo speed ω_t.

The mass flow is modeled by solving Φ_c from Eq. (65) and solving W_c from Eq. (64).

$$\Phi_c = \sqrt{\frac{1 - c_{\Psi 1}\,(\Psi_c - c_{\Psi 2})^2}{c_{\Phi 1}}} + c_{\Phi 2} \tag{68}$$

$$W_c = \frac{p_{amb}\,\pi\, R_c^3\, \omega_t}{R_a\, T_{amb}} \Phi_c \tag{69}$$

Tuning model parameters

- $c_{\Psi 2}$, $c_{\Phi 2}$: parameters in the ellipse model for the compressor mass flow
- $c_{\omega\Psi 1}$, $c_{\omega\Psi 2}$, $c_{\omega\Psi 3}$: coefficients in the polynomial function Eq. (66)
- $c_{\omega\Phi 1}$, $c_{\omega\Phi 2}$, $c_{\omega\Phi 3}$: coefficients in the polynomial function Eq. (67)

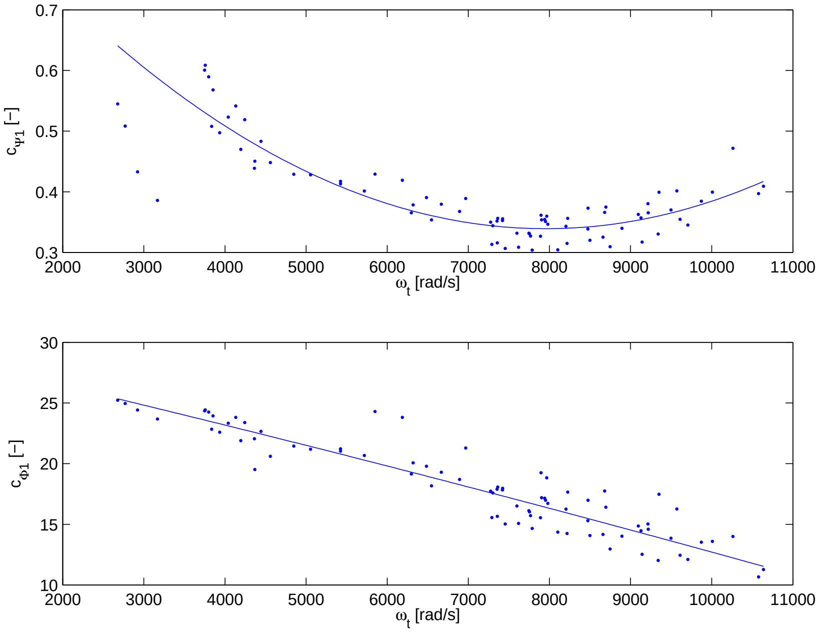

Figure 14: Comparison of estimated points from measurements and two sub-models for the compressor mass flow at steady state showing how different variables in the sub-models depend on each other. Note that this is not a validation of the sub-models since the estimated points for the sub-models depend on the model tuning. The sub-models are the ellipse variables $c_{\Psi1}$ and $c_{\Phi1}$ as function of turbo speed ω_t. The estimated points are calculated by solving $c_{\Psi1}$ and $c_{\Phi1}$ from Eq. (65). The models are described by Eq. (66) and (67).

Tuning method

The tuning parameters $c_{\Psi2}$ and $c_{\Phi2}$ are obtained by solving a non-linear least-squares problem that minimizes $(c_{\Psi1}(\omega_t)\,(\Psi_c - c_{\Psi2})^2 + c_{\Phi1}(\omega_t)\,(\Phi_c - c_{\Phi2})^2 - 1)^2$ with $c_{\Psi2}$ and $c_{\Phi2}$ as the optimization variables. In each iteration in the non-linear least-squares solver, the values for $c_{\omega\Psi1}$, $c_{\omega\Psi2}$, $c_{\omega\Psi3}$, $c_{\omega\Phi1}$, $c_{\omega\Phi2}$, and $c_{\omega\Phi3}$ are set to be the solution of a linear least-squares problem that minimizes $(c_{\Psi1}(\omega_t)\,(\Psi_c - c_{\Psi2})^2 + c_{\Phi1}(\omega_t)\,(\Phi_c - c_{\Phi2})^2 - 1)^2$ for the current values of $c_{\Psi2}$ and $c_{\Phi2}$. Stationary measurements are used as inputs to the model. The result of the tuning is shown in Fig. 15.

5.3.3 Compressor map

Compressor performance is usually presented by a map with constant efficiency lines and constant turbo speed lines and with Π_c and W_c on the axes. This is shown in Fig. 16 which has approximatively the same characteristics as Fig. 2.10 in Watson and Janota (1982). Consequently, the proposed compressor model has the expected behavior.

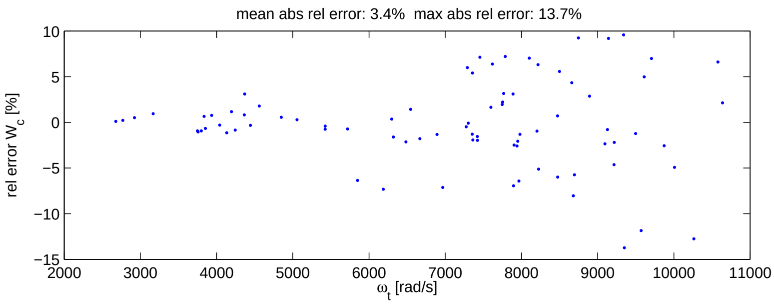

Figure 15: Relative errors for compressor flow W_c as function of turbocharger speed ω_t at steady state.

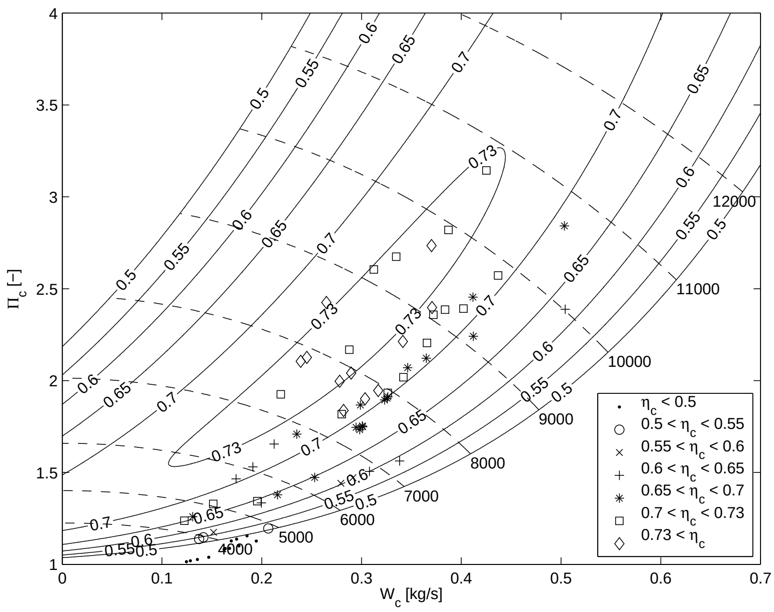

Figure 16: Compressor map with modeled efficiency lines (solid line), modeled turbo speed lines (dashed line with turbo speed in rad/s), and estimated efficiency from measurements using Eq. (55). The estimated points are divided into different groups. The turbo speed lines are described by the compressor flow model.

6 Intercooler and EGR-cooler

To construct a simple model, that captures the important system properties, the intercooler and the EGR-cooler are assumed to be ideal, i.e. the equations for the coolers are

$$
\begin{aligned}
p_{out} &= p_{in} \\
W_{out} &= W_{in} \\
T_{out} &= T_{cool}
\end{aligned}
\tag{70}
$$

where T_{cool} is the cooling temperature. The model can be extended with non-ideal coolers, but these increase the complexity of the model since non-ideal coolers require that there are states for the pressures both before and after the coolers.

7 Summary of assumptions and model equations

A summary of the model assumptions is given in Sec. 7.1 and the proposed model equations are given in Sec. 7.2 to 7.5.

7.1 Assumptions

To develop a simple model, that captures the dominating effects in the mass flows, the following assumptions are made:

- The intercooler and the EGR-cooler are ideal, i.e. the equations for the coolers are

$$\begin{aligned} p_{out} &= p_{in} \\ W_{out} &= W_{in} \\ T_{out} &= T_{cool} \end{aligned} \tag{71}$$

  where T_{cool} is the cooling temperature.

- The manifolds are modeled as standard isothermal models.
- All gases are considered to be ideal and there are two sets of thermodynamic properties:
  1. Air has the gas constant R_a and the specific heat capacity ratio γ_a.
  2. Exhaust gas has the gas constant R_e and the specific heat capacity ratio γ_e.
- No heat transfer to or from the gas inside of the intake manifold.
- No backflow can occur.
- The intake manifold temperature is constant.
- The oxygen fuel ratio λ_O is always larger than one.

7.2 Manifolds

$$\begin{aligned} \frac{d}{dt}\, p_{im} &= \frac{R_a\, T_{im}}{V_{im}}\,(W_c + W_{egr} - W_{ei}) \\ \frac{d}{dt}\, p_{em} &= \frac{R_e\, T_{em}}{V_{em}}\,(W_{eo} - W_t - W_{egr}) \end{aligned} \tag{72}$$

$$x_{egr} = \frac{W_{egr}}{W_c + W_{egr}} \tag{73}$$

$$\begin{aligned} \frac{d}{dt}\, X_{Oim} &= \frac{R_a\, T_{im}}{p_{im}\, V_{im}}\,((X_{Oem} - X_{Oim})\, W_{egr} + (X_{Oc} - X_{Oim})\, W_c) \\ \frac{d}{dt}\, X_{Oem} &= \frac{R_e\, T_{em}}{p_{em}\, V_{em}}\,(X_{Oe} - X_{Oem})\, W_{eo} \end{aligned} \tag{74}$$

7.3 Cylinder

7.3.1 Cylinder flow

$$W_{ei} = \frac{\eta_{vol}\, p_{im}\, n_e\, V_d}{120\, R_a\, T_{im}} \tag{75}$$

$$\eta_{vol} = c_{vol1}\sqrt{p_{im}} + c_{vol2}\sqrt{n_e} + c_{vol3} \tag{76}$$

$$W_f = \frac{10^{-6}}{120}\, u_\delta\, n_e\, n_{cyl} \tag{77}$$

$$W_{eo} = W_f + W_{ei} \tag{78}$$

$$\lambda_O = \frac{W_{ei}\, X_{Oim}}{W_f\, (O/F)_s} \tag{79}$$

$$X_{Oe} = \frac{W_{ei}\, X_{Oim} - W_f\, (O/F)_s}{W_{eo}} \tag{80}$$

7.3.2 Cylinder out temperature

$$\begin{aligned}
q_{in,k+1} &= \frac{W_f\, q_{HV}}{W_{ei} + W_f}\,(1 - x_{r,k}) \\
x_{p,k+1} &= 1 + \frac{q_{in,k+1}\, x_{cv}}{c_{va}\, T_{1,k}\, r_c^{\gamma_a - 1}} \\
x_{v,k+1} &= 1 + \frac{q_{in,k+1}\,(1 - x_{cv})}{c_{pa}\left(\frac{q_{in,k+1}\, x_{cv}}{c_{va}} + T_{1,k}\, r_c^{\gamma_a - 1}\right)} \\
x_{r,k+1} &= \frac{\Pi_e^{1/\gamma_a}\, x_{p,k+1}^{-1/\gamma_a}}{r_c\, x_{v,k+1}} \\
T_{e,k+1} &= \eta_{sc}\, \Pi_e^{1-1/\gamma_a}\, r_c^{1-\gamma_a}\, x_{p,k+1}^{1/\gamma_a - 1}\left(q_{in,k+1}\left(\frac{1 - x_{cv}}{c_{pa}} + \frac{x_{cv}}{c_{va}}\right) + T_{1,k}\, r_c^{\gamma_a - 1}\right) \\
T_{1,k+1} &= x_{r,k+1}\, T_{e,k+1} + (1 - x_{r,k+1})\, T_{im}
\end{aligned} \tag{81}$$

$$T_{em} = T_{amb} + (T_e - T_{amb})\, e^{-\frac{h_{tot}\, \pi\, d_{pipe}\, l_{pipe}\, n_{pipe}}{W_{eo}\, c_{pe}}} \tag{82}$$

7.3.3 Cylinder torque

$$M_e = M_{ig} - M_p - M_{fric} \tag{83}$$

$$M_p = \frac{V_d}{4\,\pi}\,(p_{em} - p_{im}) \tag{84}$$

$$M_{ig} = \frac{u_\delta\, 10^{-6}\, n_{cyl}\, q_{HV}\, \eta_{ig}}{4\,\pi} \tag{85}$$

$$\eta_{ig} = \eta_{igch}\left(1 - \frac{1}{r_c^{\gamma_{cyl} - 1}}\right) \tag{86}$$

$$M_{fric} = \frac{V_d}{4\,\pi} 10^5\,\left(c_{fric1}\, n_{eratio}^2 + c_{fric2}\, n_{eratio} + c_{fric3}\right) \tag{87}$$

$$n_{eratio} = \frac{n_e}{1000} \tag{88}$$

7.4 EGR-valve

$$W_{egr} = \frac{A_{egr}\, p_{em}\, \Psi_{egr}}{\sqrt{T_{em}\, R_e}} \tag{89}$$

$$\Psi_{egr} = 1 - \left(\frac{1 - \Pi_{egr}}{1 - \Pi_{egropt}} - 1 \right)^2 \tag{90}$$

$$\mathit{\Pi}_{egr} = \begin{cases} \Pi_{egropt} & \text{if } \frac{p_{im}}{p_{em}} < \Pi_{egropt} \\ \frac{p_{im}}{p_{em}} & \text{if } \Pi_{egropt} \le \frac{p_{im}}{p_{em}} \le 1 \\ 1 & \text{if } 1 < \frac{p_{im}}{p_{em}} \end{cases} \tag{91}$$

$$A_{egr} = A_{egrmax}\, f_{egr}(\tilde{u}_{egr}) \tag{92}$$

$$f_{egr}(\tilde{u}_{egr}) = \begin{cases} c_{egr1}\, \tilde{u}_{egr}^2 + c_{egr2}\, \tilde{u}_{egr} + c_{egr3} & \text{if } \tilde{u}_{egr} \le -\frac{c_{egr2}}{2\, c_{egr1}} \\ c_{egr3} - \frac{c_{egr2}^2}{4\, c_{egr1}} & \text{if } \tilde{u}_{egr} > -\frac{c_{egr2}}{2\, c_{egr1}} \end{cases} \tag{93}$$

$$\frac{d}{dt}\, \tilde{u}_{egr} = \frac{1}{\tau_{egr}} (u_{egr}(t - \tau_{degr}) - \tilde{u}_{egr}) \tag{94}$$

7.5 Turbo

7.5.1 Turbo inertia

$$\frac{d}{dt} \omega_t = \frac{P_t\, \eta_m - P_c}{J_t\, \omega_t} \tag{95}$$

7.5.2 Turbine efficiency

$$P_t\, \eta_m = \eta_{tm}\, W_t\, c_{pe}\, T_{em} \left(1 - \Pi_t^{1-1/\gamma_e} \right) \tag{96}$$

$$\Pi_t = \frac{p_{amb}}{p_{em}} \tag{97}$$

$$\eta_{tm} = \eta_{tm,max} - c_m (BSR - BSR_{opt})^2 \tag{98}$$

$$BSR = \frac{R_t\, \omega_t}{\sqrt{2\, c_{pe}\, T_{em} \left(1 - \Pi_t^{1-1/\gamma_e} \right)}} \tag{99}$$

$$c_m = c_{m1} (\omega_t - c_{m2})^{c_{m3}} \tag{100}$$

7.5.3 Turbine mass flow

$$W_t = \frac{A_{vgtmax}\, p_{em}\, f_{\Pi t}(\Pi_t)\, f_{vgt}(\tilde{u}_{vgt})}{\sqrt{T_{em}}} \tag{101}$$

$$f_{\Pi t}(\Pi_t) = \sqrt{1 - \Pi_t^{K_t}} \tag{102}$$

$$f_{vgt}(\tilde{u}_{vgt}) = c_{f2} + c_{f1} \sqrt{1 - \left(\frac{\tilde{u}_{vgt} - c_{vgt2}}{c_{vgt1}} \right)^2} \tag{103}$$

$$\frac{d}{dt}\, \tilde{u}_{vgt} = \frac{1}{\tau_{vgt}} (u_{vgt} - \tilde{u}_{vgt}) \tag{104}$$

7.5.4 Compressor efficiency

$$P_c = \frac{W_c\, c_{pa}\, T_{amb}}{\eta_c} \left(\Pi_c^{1-1/\gamma_a} - 1 \right) \tag{105}$$

$$\Pi_c = \frac{p_{im}}{p_{amb}} \tag{106}$$

$$\eta_c = \eta_{cmax} - \chi^T\, Q_c\, \chi \tag{107}$$

$$\chi = \begin{bmatrix} W_c - W_{copt} \\ \pi_c - \pi_{copt} \end{bmatrix} \tag{108}$$

$$\pi_c = (\Pi_c - 1)^{pow_\pi} \tag{109}$$

$$Q_c = \begin{bmatrix} a_1 & a_3 \\ a_3 & a_2 \end{bmatrix} \tag{110}$$

7.5.5 Compressor mass flow

$$W_c = \frac{p_{amb}\, \pi\, R_c^3\, \omega_t}{R_a\, T_{amb}} \Phi_c \tag{111}$$

$$\Phi_c = \sqrt{\frac{1 - c_{\Psi 1} \left(\Psi_c - c_{\Psi 2} \right)^2}{c_{\Phi 1}}} + c_{\Phi 2} \tag{112}$$

$$\Psi_c = \frac{2\, c_{pa}\, T_{amb} \left(\Pi_c^{1-1/\gamma_a} - 1 \right)}{R_c^2\, \omega_t^2} \tag{113}$$

$$c_{\Psi 1} = c_{\omega \Psi 1}\, \omega_t^2 + c_{\omega \Psi 2}\, \omega_t + c_{\omega \Psi 3} \tag{114}$$

$$c_{\Phi 1} = c_{\omega \Phi 1}\, \omega_t^2 + c_{\omega \Phi 2}\, \omega_t + c_{\omega \Phi 3} \tag{115}$$

8 Model tuning and validation

To develop a model that describes the system dynamics and the nonlinear effects, the model have to be tuned and validated. In Sec. 8.1 static and dynamic models are tuned and in Sec. 8.2 a validation of the complete model is performed using dynamic data. In the validation, it is important to investigate if the model captures the essential dynamic behaviors and nonlinear effects.

8.1 Tuning

The tuning of static and dynamic models are described in the following sections.

Static models

In Tab. 3 there is a summary of the absolute relative model errors from Sec. 3 to 5 between static models and stationary measurements for each subsystem. The stationary measurements consist of 82 operating points, that are scattered over a large operating region with different loads, speeds, VGT- and EGR-positions. These 82 operating points also include the European Stationary Cycle (ESC). The mean absolute relative errors are equal to or lower than 6.1 %. The EGR mass flow model has the largest mean relative error and the cylinder mass flow model has the smallest mean relative error.

Table 3: The mean and maximum absolute relative errors between static models and steady state measurements for each subsystem in the diesel engine model, i.e. a summary of the mean and maximum absolute relative errors in Sec. 3 to 5.

Subsystem	Mean absolute relative error [%]	Maximum absolute relative error [%]
Cylinder mass flow	0.9	2.5
Exhaust gas temperature	1.7	5.4
Engine torque	1.9	7.1
EGR mass flow	6.1	22.2
Turbine efficiency	4.2	13.2
Turbine mass flow	2.8	7.6
Compressor efficiency	3.3	14.1
Compressor mass flow	3.4	13.7

Dynamic models

The tuning parameters for the dynamic models are the manifold volumes V_{im} and V_{em} in Sec. 2 and the turbo inertia J_t in Sec. 5.1. These parameters are adjusted manually until simulations of the complete model follow dynamic responses in dynamic measurements by considering time constants. The tuning is performed using a dynamic tuning data, the data C in Tab. 4, that consists of 77 different steps in VGT control signal and EGR control signal in an operating point with 50 % load and n_e=1500 rpm. All the data in Tab. 4 are used for validation in Sec. 8.2. Note that the dynamic measurements are limited in sample rate with a sample frequency of 1 Hz for data A-E and with a sample

Table 4: The mean absolute relative errors between diesel engine model simulation and dynamic tuning or validation data that consist of steps in VGT-position, EGR-valve, and fuel injection. The data C and F are used for tuning of dynamic models, the data A, B, D, E, and F are used for validation of time constants, and all the data are used for validation of static models and essential system properties.

	VGT-EGR steps					u_δ steps
Data name	A	B	C	D	E	F
Speed [rpm]	1200		1500	1900		1500
Load [%]	25	75	50	25	75	-
Number of steps	77	77	77	77	55	7
p_{im}	2.0	10.6	6.3	5.0	4.5	2.9
p_{em}	2.4	6.8	5.5	4.5	4.6	4.7
W_c	3.2	10.6	8.0	6.7	6.7	3.8
n_t	4.4	11.9	7.0	6.0	4.1	3.0
M_e	-	-	-	-	-	7.3

frequency of 10 Hz for data F. This leads to that the data does not captures the fastest dynamics in the system.

A dynamometer is fitted to the engine via an axle in order to brake or supply torque to the engine. This dynamometer and axle lead to that the measured engine torque has a time constant that is not modeled due to that the torque will not be used as a feedback in the controller. However, in order to validate the engine torque model during dynamic responses, this dynamic is modeled in the validation as a first order system

$$\frac{d}{dt} M_{e,meas} = \frac{1}{\tau_{Me}}(M_e - M_{e,meas}) \tag{116}$$

where $M_{e,meas}$ is the measured torque and M_e is the output torque from the engine. The time constant τ_{Me} is tuned by adjusting it manually until simulations of the complete model follow the measured torque during steps in fuel injection at 1500 rpm, i.e. the data F in Tab. 4.

8.2 Validation

Due to that the stationary measurements are few, both the static and the dynamic models are validated by simulating the total model and comparing it with dynamic validation data that consists of several different steps in VGT-position, EGR-valve, and fuel injection. The steps in VGT-position and EGR-valve are performed in 5 different operating points and the steps in fuel injection are performed in one operating point. The result of this validation can be seen in Tab. 4 that shows that the mean absolute relative errors are less than 12 %. Note that the engine torque is not measured during VGT and EGR steps. The relative errors are due to mostly steady state errors, but since the engine model will be used in a controller the steady state accuracy is less important since a controller will take care of steady state errors. However, in order to design a successful controller, it is important that the model captures the essential dynamic behaviors and nonlinear effects. Therefore, time constants and essential system properties are validated in the following sections.

Validation of time constants

In Sec. 8.1, the dynamic models are tuned by considering the time constants in the data C in Tab. 4. These time constants are validated using the dynamic validation data A, B, D, and E in Tab. 4. Some parts of this validation are plotted in Fig. 17 and 18. The non-minimum phase behavior in p_{im} in Fig. 17 shows that the model captures the fast dynamic in the beginning of the response and that the model captures the slow dynamic in the end of the response. The overshoot in the third response in Fig. 18 also shows that model captures both fast and slow dynamics.

Validation of essential system properties

Kolmanovsky et al. (1997) and Jung (2003) show the essential system properties for the pressures and the flows in a diesel engine with VGT and EGR. Some of these properties are a non-minimum phase behavior in the intake manifold pressure and a non-minimum phase behavior, an overshoot, and a sign reversal in the compressor mass flow. These system properties are validated using the dynamic data A-E in Tab. 4. Some parts of this validation are shown in Fig. 17 to 19. Fig. 17 shows that the model captures the non-minimum phase behavior in the transfer function u_{egr} to p_{im} and the second step in Fig. 19 shows that the model captures the non-minimum phase behavior in the transfer function u_{vgt} to W_c. Note that the non-minimum phase behaviors in the measurements are not obvious due to a low sample frequency. Further, the third step in Fig. 18 and the third step in Fig. 19 show that the model captures the overshoot and the sign reversal in the transfer function u_{vgt} to W_c.

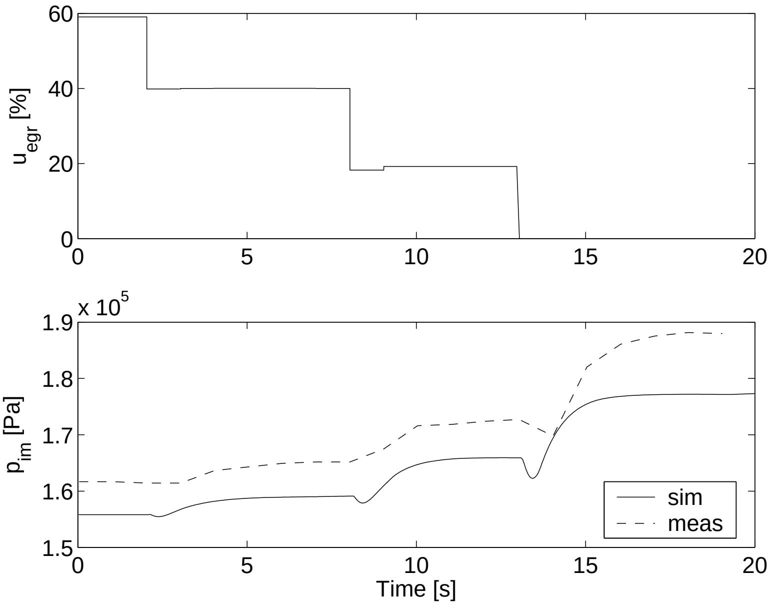

Figure 17: Comparison between diesel engine model simulation and dynamic validation data during steps in EGR-valve position showing that the model captures the non-minimum phase behavior in p_{im}. Operating point: 25 % load, n_e=1900 rpm and u_{vgt}=50 %.

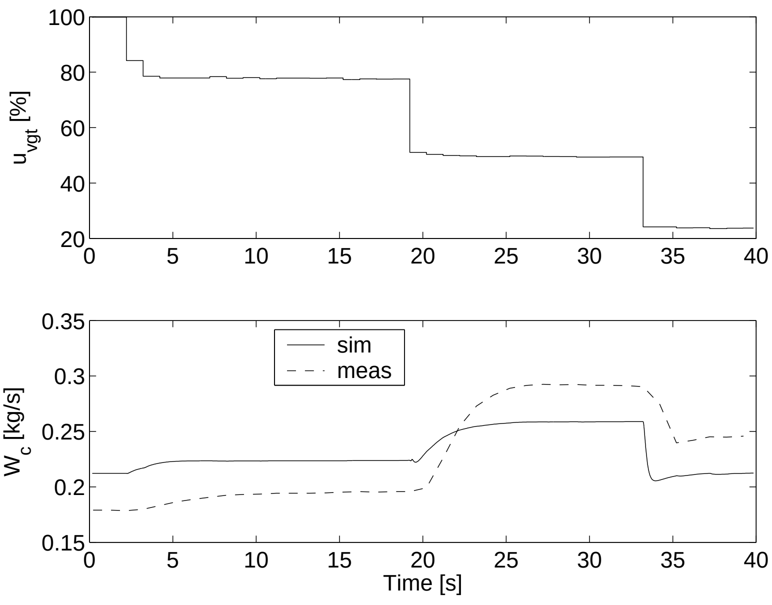

Figure 18: Comparison between diesel engine model simulation and dynamic validation data during steps in VGT position showing that the model captures the overshoot and the sign reversal in W_c. Operating point: 75 % load, n_e=1200 rpm and u_{egr}=40 %.

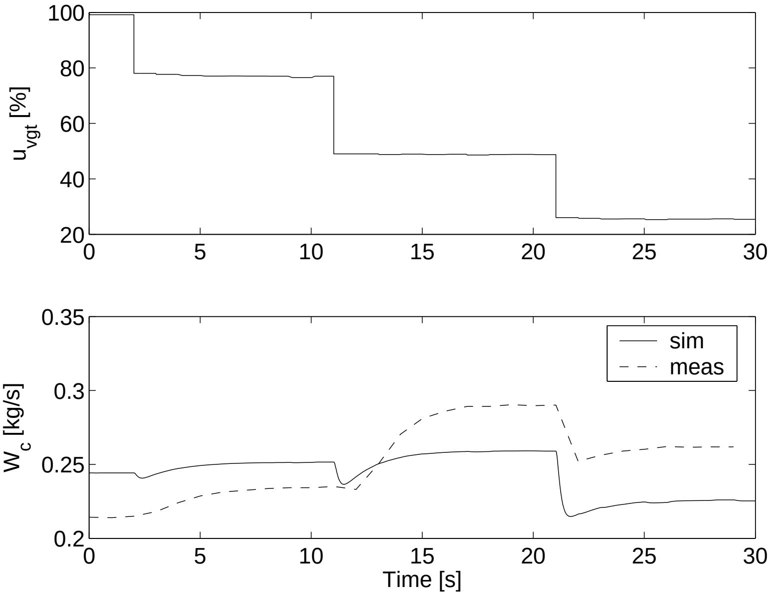

Figure 19: Comparison between diesel engine model simulation and dynamic tuning data during steps in VGT position showing that the model captures the non-minimum phase behavior, the overshoot, and the sign reversal in W_c. Operating point: 50 % load, n_e=1500 rpm and u_{egr}=81.5 %.

9 Conclusions

A mean value model of a diesel engine with VGT and EGR including oxygen mass fraction was developed and validated. The intended applications of the model are system analysis, simulation, and development of model-based control systems. To be able to implement a model-based controller, the model must be small. Therefore the model has only seven states: intake and exhaust manifold pressures, oxygen mass fraction in the intake and exhaust manifold, turbocharger speed, and two states describing the actuator dynamics for the EGR-valve and the VGT-position.

Model equations and tuning methods for the model parameters was described for each subsystem in the model. Parameters in the static models are tuned automatically using least square optimization and stationary measurements in 82 different operating points. The tuning shows that the mean relative errors are equal to or lower than 6.1 %. Parameters in dynamic models are tuned by adjusting these parameters manually until simulations of the complete model follow the dynamic responses in the dynamic measurements. In order to decrease the amount of tuning parameters, flows and efficiencies are modeled using physical relationships and parametric models instead of look-up tables.

Static and dynamic validations of the entire model were performed using dynamic measurements, which consist of steps in fuel injection, EGR control signal, and VGT control signal. The validations show mean relative errors which are less than 12 %. The validations also show that the proposed model captures the essential system properties, i.e. a non-minimum phase behavior in the transfer function u_{egr} to p_{im} and a non-minimum phase behavior, an overshoot, and a sign reversal in the transfer function u_{vgt} to W_c.

References

Andersson, P. (2005). *Air Charge Estimation in Turbocharged Spark Ignition Engines.* PhD thesis, Linköpings Universitet.

Dixon, S. (1998). *Fluid Mechanics and Thermodynamics of Turbomachinery.* Butterworth Heinemann, Woburn, 4:th edition.

Eriksson, L. (2002). Mean value models for exhaust system temperatures. *SAE 2002 Transactions, Journal of Engines, 2002-01-0374*, 111(3).

Eriksson, L., Nielsen, L., Brugård, J., Bergström, J., Pettersson, F., and Andersson, P. (2002). Modeling and simulation of a turbo charged SI engine. *Annual Reviews in Control*, 26(1):129–137.

Guzzella, L. and Amstutz, A. (1998). Control of diesel engines. *IEEE Control Systems Magazine*, 18:53–71.

Heywood, J. (1988). *Internal Combustion Engine Fundamentals.* McGraw-Hill Book Co.

Jung, M. (2003). *Mean-Value Modelling and Robust Control of the Airpath of a Turbocharged Diesel Engine.* PhD thesis, University of Cambridge.

Kolmanovsky, I., Stefanopoulou, A., Moraal, P., and van Nieuwstadt, M. (1997). Issues in modeling and control of intake flow in variable geometry turbocharged engines. In *Proceedings of* 18^{th} *IFIP Conference on System Modeling and Optimization*, Detroit.

Skogtjärn, P. (2002). Modelling of the exhaust gas temperature for diesel engines. Master's thesis LiTH-ISY-EX-3379, Department of Electrical Engineering, Linköping University, Linköping, Sweden.

Vigild, C. (2001). *The Internal Combustion Engine Modelling, Estimation and Control Issues.* PhD thesis, Technical University of Denmark, Lyngby.

Watson, N. and Janota, M. (1982). *Turbocharging the Internal Combustion Engine.* The Mechanical Press Ltd, Hong Kong.

A Notation

Table 5: Symbols used in the report

Symbol	Description	Unit
A	Area	m^2
BSR	Blade speed ratio	$-$
c_p	Spec. heat capacity, constant pressure	$J/(kg \cdot K)$
c_v	Spec. heat capacity, constant volume	$J/(kg \cdot K)$
J	Inertia	$kg \cdot m^2$
M	Torque	Nm
M_e	Engine torque	Nm
M_p	Pumping torque	Nm
n_{cyl}	Number of cylinders	$-$
n_e	Rotational engine speed	rpm
n_t	Rotational turbine speed	rpm
$(O/F)_s$	Stoichiometric oxygen-fuel ratio	$-$
p	Pressure	Pa
P	Power	W
q_{HV}	Heating value of fuel	J/kg
r_c	Compression ratio	$-$
R	Gas constant	$J/(kg \cdot K)$
R	Radius	m
T	Temperature	K
u_{egr}	EGR control signal. 100 - open, 0 - closed	%
u_{vgt}	VGT control signal. 100 - open, 0 - closed	%
u_δ	Injected amount of fuel	$mg/cycle$
V	Volume	m^3
W	Mass flow	kg/s
x_{egr}	EGR fraction	$-$
X_O	Oxygen mass fraction	$-$
γ	Specific heat capacity ratio	$-$
η	Efficiency	$-$
λ_O	Oxygen-fuel ratio	$-$
Π	Pressure quotient	$-$
ρ	Density	kg/m^3
τ	Time constant	s
Φ_c	Volumetric flow coefficient	$-$
Ψ_c	Energy transfer coefficient	$-$
ω	Rotational speed	rad/s

Table 6: Indices used in the report

Index	Description
a	air
amb	ambient
c	compressor
d	displaced
e	exhaust
egr	EGR
ei	engine cylinder in
em	exhaust manifold
eo	engine cylinder out
f	fuel
$fric$	friction
ig	indicated gross
im	intake manifold
m	mechanical
t	turbine
vgt	VGT
vol	volumetric
δ	fuel injection

Table 7: Abbreviations used in the report

Abbreviation	Description
EGR	Exhaust gas recirculation
VGT	Variable geometry turbocharger